Strain-Driven Approach to Quantum Criticality in $A\mathrm{Fe_2As_2}$ with $A = \mathrm{K}$, Rb, and Cs

Felix Eilers,[1] Kai Grube,[1] Diego A. Zocco,[1] Thomas Wolf,[1] Michael Merz,[1] Peter Schweiss,[1] Rolf Heid,[1] Robert Eder,[1] Rong Yu,[2] Jian-Xin Zhu,[3] Qimiao Si,[4] Takasada Shibauchi,[5,6] and Hilbert v. Löhneysen[1,7]

[1]*Institut für Festkörperphysik, Karlsruher Institut für Technologie, 76021 Karlsruhe, Germany*
[2]*Department of Physics, Renmin University of China, Beijing 100872, China*
[3]*Theoretical Division, Los Alamos National Laboratory, Los Alamos, New Mexico 87545, USA*
[4]*Department of Physics and Astronomy, Rice University, Houston, Texas 77005, USA*
[5]*Department of Advanced Materials Science, University of Tokyo, Kashiwa, Chiba 277-8561, Japan*
[6]*Department of Physics, Kyoto University, Sakyo-ku, Kyoto 606-8502, Japan*
[7]*Physikalisches Institut, Karlsruher Institut für Technologie, 76049 Karlsruhe, Germany*

(Received 7 October 2015; revised manuscript received 8 April 2016; published 8 June 2016)

The iron-based superconductors $A\mathrm{Fe_2As_2}$ with $A = \mathrm{K}$, Rb, Cs exhibit large Sommerfeld coefficients approaching those of heavy-fermion systems. We have investigated the magnetostriction and thermal expansion of this series to shed light on this unusual behavior. Quantum oscillations of the magnetostriction allow identifying the band-specific quasiparticle masses which by far exceed the band-structure derived masses. The divergence of the Grüneisen ratio derived from thermal expansion indicates that with increasing volume along the series a quantum critical point is approached. The critical fluctuations responsible for the enhancement of the quasiparticle masses appear to weaken the superconducting state.

DOI: 10.1103/PhysRevLett.116.237003

Unconventional superconductivity (SC) often emerges in the proximity of continuous, zero-temperature phase transitions, so-called quantum critical points (QCPs). In particular, the onset of magnetic order is generally believed to drive SC by magnetic quantum criticality. Examples encompass the cuprates, organic metals, heavy-fermion systems, and the recently discovered iron-based superconductors. A particularly illustrative example is given by $\mathrm{BaFe_2}(\mathrm{As}_{1-x}\mathrm{P}_x)_2$. Here, the application of chemical pressure, by replacing As with isovalent, smaller P ions, suppresses antiferromagnetic (AFM) order resulting in an extended superconducting dome with a maximum transition temperature $T_c \approx 30$ K at the critical concentration $x_c = 0.3$ [1]. The QCP at x_c shielded by SC was anticipated theoretically [2] and observed through strongly enhanced quasiparticle masses and deviations from Fermi-liquid (FL) behavior. In this Letter, we show that the isostructural superconductor $\mathrm{KFe_2As_2}$ can likewise be pushed towards a QCP by substituting isovalent, but larger Rb and Cs for K. In these compounds, in contrast to the examples listed above and despite general consensus, quantum criticality fails to boost SC.

The alkali metal series $A\mathrm{Fe_2As_2}$ ($A122$) with $A = \mathrm{K}$, Rb, and Cs, represent one of the rare examples of stoichiometric iron-arsenide superconductors. According to local-density approximation (LDA) calculations their low-T_c values of less than 3.5 K cannot be explained by electron-phonon coupling [3]. Angle-resolved photoemission spectroscopy and thermal-conductivity measurements suggest an unconventional pairing mechanism [4–7]. Recent specific-heat measurements reveal huge Sommerfeld coefficients γ which exceed those of $\mathrm{BaFe_2}(\mathrm{As}_{1-x}\mathrm{P}_x)_2$ in apparent contradiction to the low-T_c values [7–9]. In order to elucidate the highly correlated normal state and its relationship to SC, we investigated the quantum oscillations observable in the magnetostriction of the $A122$ series.

Single-crystalline samples were grown from an arsenic-rich flux, yielding T_c values of 3.40(5), 2.53(3), and 2.27(4) K for $A = \mathrm{K}$, Rb, and Cs, respectively [10]. The low impurity concentration of the crystals allows observing quantum oscillations of the sample length as a function of the applied magnetic field B ranging between the upper critical field B_{c2} and the maximum field of 14 T (insets of Fig. 1). The mean free paths determined from the field dependence of these oscillations confirm that the decreasing T_c values in the $A122$ series do not arise from varying sample quality [10]. To extract the fundamental frequencies, we performed a Fourier transformation of the oscillatory part of the measured magnetostriction coefficient $\lambda_i \equiv L_i^{-1}\partial L_i/\partial B$, where L_i is the sample length along the tetragonal $i = a$ and c directions.

The spectra of the three $A122$ compounds taken at $T = 50$ mK for $B \| a$ and c, are plotted as amplitude against frequency F in Fig. 1. The data of K122 are taken from Refs. [28–30]. The difference between the λ_a and λ_c spectra reflects the anisotropic uniaxial pressure dependences of the Fermi-surface (FS) cross sections [31]. The observed sharp peaks mark the fundamental and higher harmonic cyclotron frequencies corresponding to the extremal orbits of the FS, which have been assigned to specific bands by comparing the spectra of Rb122 and Cs122 to those of K122 and to our LDA calculations. For $A = \mathrm{Rb}$ and Cs, all FS sheets apart from the β band could be identified. As the isovalent substitution of A keeps the total hole count

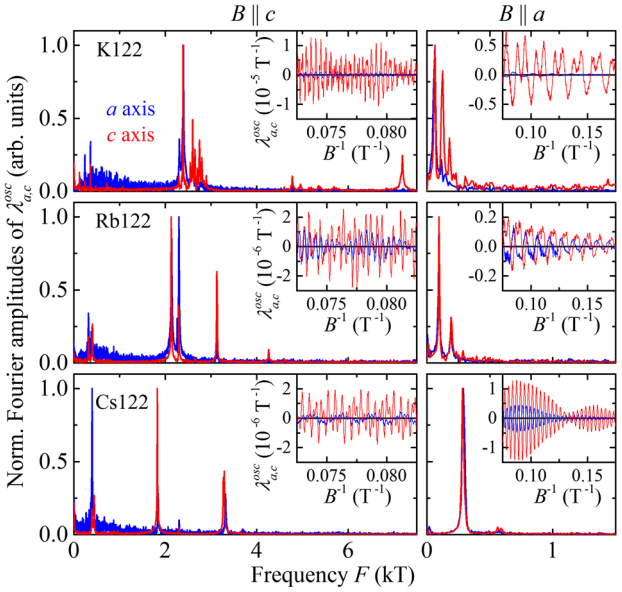

FIG. 1. Normalized Fourier spectra of the oscillatory part of the magnetostriction coefficient λ_i^{osc} (insets) along the $i = a$ (blue) and c axis (red line) of $A122$, A = K, Rb, and Cs, at $T = 50$ mK for $B\|c$ and a.

constant we can estimate the contribution of the β sheet by subtracting the cross sections of all other bands from the FS volume of K122. In Fig. 2(a) the obtained extremal cross-sectional areas, expressed as fractions of the volume of the first Brillouin zone, are plotted against the radius of the alkali-metal ion R_A.

In line with our LDA calculations, the data show no change of the FS topology with increasing R_A. The

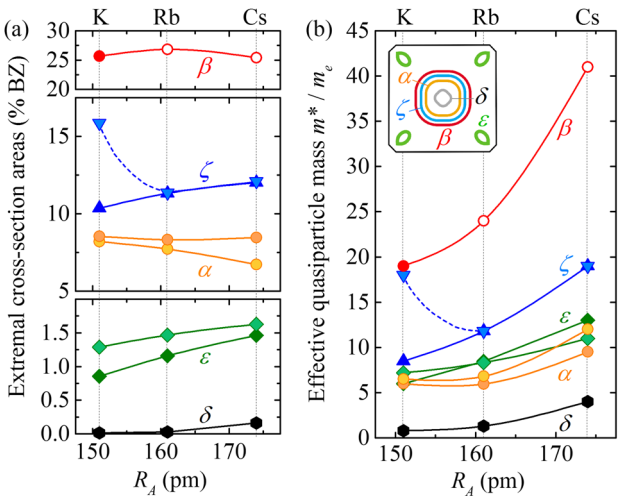

FIG. 2. (a) Extremal cross-sectional areas of the Fermi surfaces of (K,Rb,Cs)122, expressed as fractions of the first Brillouin-zone volumes. (b) Effective quasiparticle masses m^*, plotted against the ionic radius of the alkaline atom R_A [28–30]. The values presented by open symbols were obtained by assuming a constant total hole count and using the Sommerfeld coefficients [7–9]. Lines are guides to the eye.

two-dimensionality of the FeAs-layered structure is reflected by three tubes in the Brillouin-zone center [α, ζ, and β, see inset of Fig. 2(b)] and one tube at each corner (ϵ). Marginal three-dimensional features were inferred from closely spaced peaks in the Fourier spectra, indicating a gentle warping of the FS tubes, and from a single fundamental frequency for $B\|a$, attributed to a tiny pocket at the top center. So far, this pocket has been seen only in magnetostriction measurements [30].

The decay of the oscillations with increasing T [10] is used to determine the effective quasiparticle masses m_j^* of each FS sheet j. Since in quasi-two-dimensional systems the Sommerfeld coefficient is given by $\gamma \approx (\pi k_B^2 N_A a^2/3\hbar^2)\sum_j m_j^*$ (N_A is Avogadro's number), the mass of the β tube can be determined by subtracting the contributions of all other bands from the published γ values. For the warped FS tubes we simply used the average value of the effective masses assuming a sinusoidal warping. The obtained large m_β^* values alone cannot account for the absence of β-band oscillations in our measurements. The β-band FS cross section does, however, hardly depend on R_A, suggesting small uniaxial pressure effects and, therefore, further reduced $\lambda_i^{\mathrm{osc}(\beta)}$ amplitudes. Figure 2(b) summarizes the resulting quasiparticle masses as a function of R_A. Not only m_β^*, but also all effective masses exhibit significant increases with R_A, with a factor of $m_j^*(\mathrm{Cs})/m_j^*(\mathrm{K}) \approx 2$, which interestingly is similar to that of $\gamma(\mathrm{Cs})/\gamma(\mathrm{K})$. LDA calculations, on the other hand, predict band masses an order of magnitude smaller, with a comparatively slight increase towards Cs122. This difference reinforces the assumption that the huge low-temperature specific heat arises from strong electronic correlations (see below).

The negative chemical pressure exerted upon replacing K by the larger Rb or Cs ions mainly expands the c axis by pushing the FeAs layers further apart from each other. To elucidate the difference between chemical and external, hydrostatic pressure, we performed thermal-expansion measurements. In a FL, the uniaxial pressure dependence of the Sommerfeld coefficient is related to the linear thermal-expansion coefficient α_i by $\partial\gamma/\partial p_i = -(V/T)\alpha_i$, where V is the molar volume and p_i uniaxial pressure in the $i = a$, c direction. The hydrostatic pressure dependence is given by $\partial\gamma/\partial p = 2\partial\gamma/\partial p_a + \partial\gamma/\partial p_c$. Between T_c and 4 K, all three compounds show FL behavior, i.e., constant α_i/T values, similarly to the published C/T data. With increasing R_A and, consequently, growing unit-cell volume, the pressure dependence decreases from $\partial\gamma/\partial p = -20.3$ mJ/mol K^2 GPa (K) [32] to -36.6 mJ/mol K^2 GPa (Rb) and -77.7 mJ/mol K^2 GPa (Cs) suggesting a nonlinear V dependence of γ. In order to compare with the chemical pressure effect, we convert the hydrostatic pressure dependences from our thermal expansion measurements to volume derivatives $\partial\gamma/\partial V = -V^{-1}B_T\partial\gamma/\partial p$, and estimate $\gamma_p(V)$ by integrating over the obtained $\partial\gamma(V)/\partial V$ values. Here, $B_T = -V\partial p/\partial V$ is the bulk

modulus. The integration constant is provided by the published γ values of K122. In a first step we take V to be the unit-cell volume V_{UC} using $B_T(V_{\mathrm{UC}}) \approx 40$ GPa of K122 [33]. The calculated $\gamma_p(V_{\mathrm{UC}})$ curves are displayed in Fig. 3(a) together with the Sommerfeld coefficients $\gamma(V_{\mathrm{UC}})$ at ambient pressure [7–9,34]. Obviously, $\gamma_p(V_{\mathrm{UC}})$ strongly overestimates the chemical pressure effect $\gamma(V_{\mathrm{UC}})$. In this simple estimate we have neglected that chemical and hydrostatic pressures affect the crystal structure in different ways: while the latter leads to a reduction or increase of *all* bond lengths, the alkali-metal substitution changes c and FeAs-layer thickness h_{FeAs} with opposite trends: it increases c and decreases h_{FeAs} [10]. Therefore, in a second step, we perform the comparison on the basis of the FeAs-cell volume $V_{\mathrm{FeAs}} = a^2 h_{\mathrm{FeAs}}$. The related bulk modulus of $B_T(V_{\mathrm{FeAs}}) \approx 145$ GPa was inferred from the high-pressure data of K122 [33]. The estimated $\gamma_p(V_{\mathrm{FeAs}})$ curves are likewise shown in Fig. 3(a). Taking V_{FeAs} as the decisive p-dependent volume, hydrostatic and chemical pressure dependences coincide with each other. This agreement suggests that the enhanced correlations originate from a change of the direct Fe environment due to a reduced hybridization of the Fe $3d$ states with nearest-neighbor Fe or As orbitals.

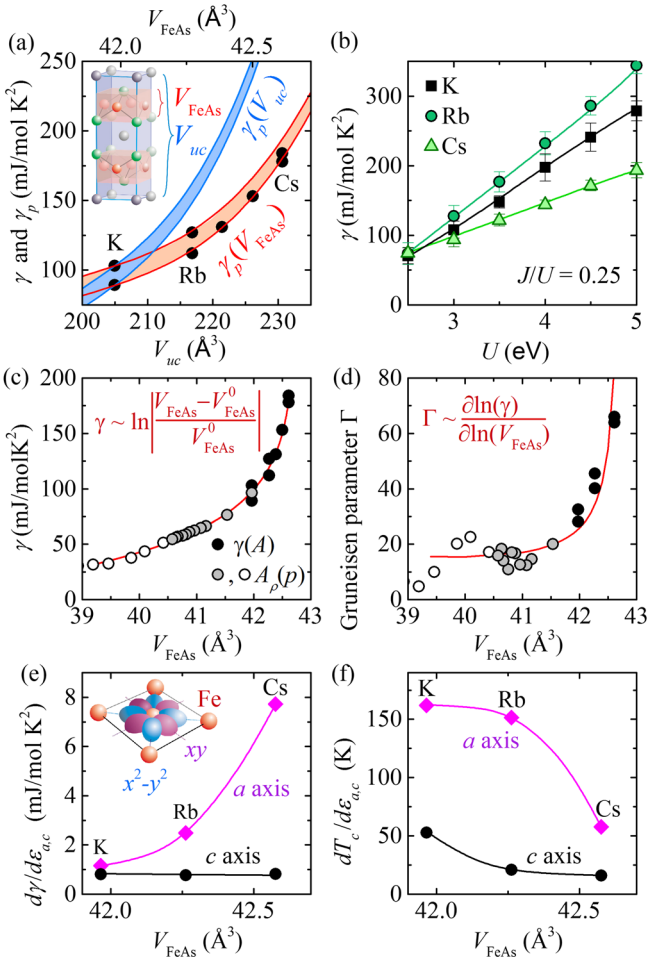

FIG. 3. (a) Comparison between chemical (black dots) and hydrostatic pressure dependences of the Sommerfeld coefficient γ as a function of the unit-cell volume V_{UC} and that of a single FeAs layer V_{FeAs}. The hydrostatic pressure dependences are extracted from the volume thermal expansion α_V for $V = V_{\mathrm{UC}}$ (blue lines) and V_{FeAs} (red lines). (b) The calculated γ as a function of U in a multiorbital Hubbard model for $A122$ (A = K, Rb, Cs) (see text). (c) Evolution of the measured γ with increasing V_{FeAs}. Gray [35] and open dots [36] are estimated from high-pressure resistivity measurements. The red line is a fit to the data points. (d) The Grüneisen parameter Γ, calculated from γ, A_ρ, and α_V. The red line is determined with the fit shown in (d) under the assumption of a Fermi liquid. (e) Strain dependences of γ and (f) the superconducting transition temperature T_c. Lines are guides to the eyes. The inset in (e) shows the Fe plane with the $3d_{xy}$ and $3d_{x^2-y^2}$ orbitals.

The role of the FeAs-cell volume was pointed out in recent publications [37–41], and provides the basis to study the evolution of electronic correlations in a wider phase space. We extended the pressure dependence of γ to smaller V_{FeAs} values by resorting to resistivity measurements of K122 under hydrostatic pressure [35,36]. Since the FL state of K122 follows the Kadowaki-Woods (KW) relation [42] we relate γ to the scattering cross section A_ρ of the low-temperature resistivity $\rho = \rho_0 + A_\rho T^2$ by using a proportionality factor of $A_\rho/\gamma^2 \approx 2 \times 10^{-6}\ \mu\Omega\,\mathrm{cm(K\,mol/mJ)^2}$ so that the ambient pressure measurements are reproduced [42]. The extended $\gamma(V_{\mathrm{FeAs}})$ data displayed in Fig. 3(c) exhibit the characteristic sudden increase of a system that is tuned towards a QCP. The best fit to this mass divergence is given by a logarithmic volume dependence $\gamma \propto \ln(|V_{\mathrm{FeAs}} - V^0_{\mathrm{FeAs}}|/V^0_{\mathrm{FeAs}})$, with $V^0_{\mathrm{FeAs}} = 42.72$ Å^3, as proposed for a two-dimensional FL close to a Mott transition and found for $BaFe_2(As_{1-x}P_x)_2$ [43].

QCPs are characterized by a vanishing characteristic energy scale E^*, leading to a divergence of the Grüneisen parameter $\Gamma \approx -d\ln(E^*)/\ln(V)$ for a pressure-induced QCP. We calculated $\Gamma = V_{\mathrm{FeAs}} B_T(V_{\mathrm{FeAs}}) \alpha_V/\gamma$ from our thermal expansion data $\alpha_V = 2\alpha_a + \alpha_c$. For the high-pressure resistivity measurements we use $\Gamma = d\ln(\gamma)/d\ln(V_{\mathrm{FeAs}}) = (1/2)d\ln(A_\rho)/d\ln(V_{\mathrm{FeAs}})$ by virtue of the KW relation. The volume dependence of Γ, shown in Fig. 3(d), clearly exhibits a pronounced divergence. This provides [44,45] clear evidence that with increasing R_A a QCP is approached and Cs122 is in its close proximity. Recent resistivity measurements of Cs122 do report indications of non-FL behavior [6].

To specify the hybridized orbitals responsible for the critical mass enhancement, we determine the uniaxial pressure dependences $\partial\gamma/\partial p_i$ for $i = a,\ c$ from α_i. Furthermore, we approximate the elastic constants c_{ij} of the $A122$ compounds by density-functional theory calculations [10] to obtain an estimate of the strain dependences $d\gamma/d\epsilon_i = \sum c_{ij} d\gamma/dp_j$. The $d\gamma/d\epsilon_i$ values show that with increasing V_{FeAs}, mainly a-axis changes account for the mass enhancement [Fig. 3(e)]. In particular, the divergence

can be observed only in $d\gamma/d\epsilon_a$. This allows identifying the orbitals involved, as in the FeAs-cell volume, only the Fe $3d_{xy}$ or $3d_{x^2-y^2}$ orbitals are confined to the ab plane [inset of Fig. 3(e)] and are, therefore, affected by a- or b-axis changes. Since the band-specific masses shown in Fig. 2 reveal the heaviest masses for the β bands with dominating d_{xy} character, we conclude that the critical mass enhancement can be attributed to the hybridization of the in-plane d_{xy} orbitals.

If, as suggested, in the traditional QCP scenario SC is supported by critical fluctuations arising close to a QCP, the strain dependence $\partial T_c/\partial\epsilon_i$ should follow that of $\partial\gamma/\partial\epsilon_i$. To check this scenario, we determine the uniaxial pressure dependences of T_c by using the Ehrenfest relations with the discontinuities of α_i and C at T_c, and convert them to $\partial T_c/\partial\epsilon_i$. Similarly to $\partial\gamma/\partial\epsilon_c$, changes of the c axis hardly affect T_c [Fig. 3(f)]. Contrary to the expectation of the above scenario, however, $\partial T_c/\partial\epsilon_a$ shows a behavior opposite to that of $\partial\gamma/\partial\epsilon_a$, and decreases with increasing V_{FeAs}. This apparent dichotomy suggests that the d_{xy} states driving the mass enhancement tend to simultaneously weaken SC. Because of the minor FS variations with R_A, a change of the electronic structure and nesting conditions can hardly account for the T_c reduction.

The specific role of the Fe $3d$ levels for the electronic correlations in Fe-based superconductors reflects the Coulomb (Hubbard and Hund) interactions as well as the small crystal-electric-field splittings [39,40,46–49]. To better understand the observed mass enhancement, we study [10] the electron correlation effects in a multiorbital Hubbard model for $A122$ using a $U(1)$ slave-spin mean-field theory [50]. The details of the model and the method can be found in the Supplemental Material [10]. The $A122$ system corresponds to a $3d$-electron filling of $N = 5.5$ per Fe atom. For this filling, we identify a strongly correlated regime for a range of realistic values for U and J (Fig. S4 of Ref. [10]). In this regime, the quasiparticle spectral weights in all five Fe $3d$ orbitals are substantially reduced, and a strong orbital dependence arises. As shown in Fig. S5, the quasiparticle spectral weight of the d_{xy} orbital is most strongly reduced, correspondingly, its mass enhancement is the largest. We further calculate the Sommerfeld coefficient γ. As shown in Fig. 3(b), the calculated γ values have a magnitude similar to the experimental values. However, for fixed values of the interactions, γ does not show a strong increase across the K through Rb to Cs series. We attribute this missing contribution to an additional component of γ arising from the proximity to quantum criticality.

The emerging picture is summarized in Fig. 4 which depicts γ in the (N, V_{FeAs}) plane. The γ values of the series $Ba_xK_{1-x}Fe_2As_2$ [51], where $N = 6 - x/2$ varies from $N = 5.5$ to 6, contrast with those of $BaFe_2(As_{1-x}P_x)_2$, where $N = 6$ and V_{FeAs} changes significantly [1,52]. Both series exhibit a maximum γ_{max} close to the onset of AFM

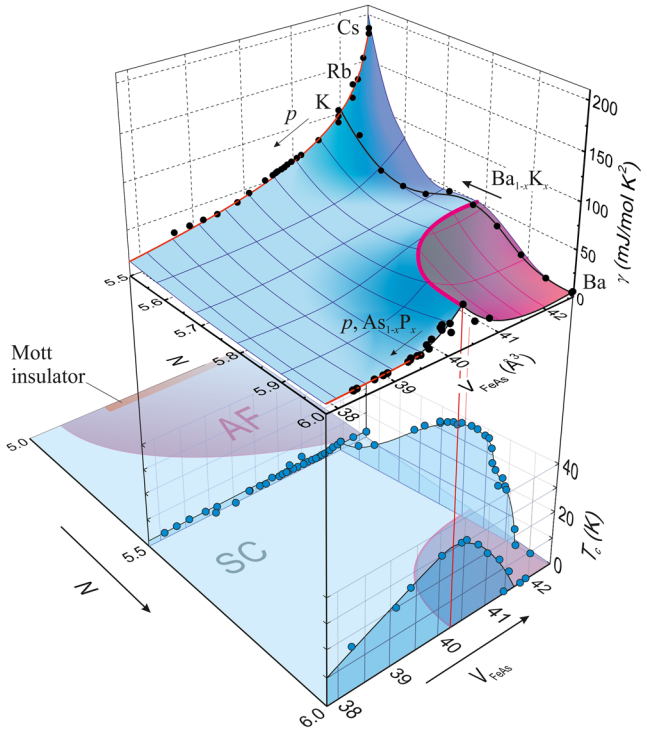

FIG. 4. Evolution of γ as a function of V_{FeAs} and hole doping expressed as filling N of the Fe $3d$ states. In addition to the high-pressure data of KFe_2As_2 [33,35,36,53], measurements of $Ba_{1-x}K_xFe_2As_2$ [51,54] and $BaFe_2(As_{1-x}P_x)_2$ [1,52,55,56] have been included. The γ values of $BaFe_2(As_{1-x}P_x)_2$ were estimated following Ref. [52]. The base plane shows a tentative phase diagram of a five-orbital Hubbard model with combined (U, J) interactions leading to a Mott-insulating state at $N = 5$ [46].

order suggesting an underlying QCP. However, the highest γ value is found for the $A122$ compounds where T_c values are one order of magnitude smaller than those of $Ba_xK_{1-x}Fe_2As_2$ and $BaFe_2(As_{1-x}P_x)_2$. Figure 4 strongly suggests that the QCP suggested by our measurements would be most naturally associated with an AFM order related to the $N = 5$ Mott-insulating phase [46].

The combined effect of Hund's rule coupling and Coulomb exchange interaction is considerably intensified by reducing the bandwidth. This is exemplified by $BaFe_2(As_{1-x}P_x)_2$ and $A122$. While in $BaFe_2(As_{1-x}P_x)_2$ the hybridization changes due to longer Fe–As bonds, in the $A122$ series only the Fe–Fe distances are widened [10,55]. Remarkably, the largest γ values are found for $A122$ with a divergent trend towards $A = \mathrm{Cs}$. These high values do not find any correspondence in the superconducting properties. In fact, it seems that here strong correlations weaken SC which might occur on rather general grounds [57,58].

We speculate that the $A122$ series might be a candidate for the special situation where a QCP exactly coincides with the onset of SC. This could provide a new insight into the physics of iron pnictides close to the $N = 5$ limit which

should be tested by investigating Cs122 films under tensile biaxial strain.

We thank Y. Mizukami, H. Ikeda, T. Terashima, P. Adelmann, F. Hardy, A. E. Böhmer, C. Meingast, J. Schmalian, L. de' Medici, M. Capone, M. Grosche, and J. Wosnitza for valuable discussions. This work has been supported by Deutsche Forschungsgemeinschaft in the frame of FOR960 (Quantum Phase Transitions) and the Japan-Germany Research Cooperative Program, KAKENHI from JSPS and Project No. 56393598 from DAAD. The work was in part supported by the U.S. DOE at LANL under Contract No. DE-AC52-06NA25396 and the DOE Office of Basic Energy Sciences (J.-X. Z.), by the National Science Foundation of China Grant No. 11374361, the Fundamental Research Funds for the Central Universities and the Research Research Funds of Renmin University of China (R. Y.), and by the NSF and the Robert A. Welch Foundation Grant No. C-1411 (Q. S.). Q. S. also acknowledges the support of the Alexander von Humboldt Foundation through a Humboldt Research Award and the hospitality of the Karlsruhe Institute of Technology. H. v. L. and Q. S. enjoyed the hospitality of the Aspen Center for Physics when finalizing the manuscript (supported by NSF Grant No. PHY-1066293).

[1] T. Shibauchi, A. Carrington, and Y. Matsuda, Annu. Rev. Condens. Matter Phys. **5**, 113 (2014).
[2] J. Dai, Q. Si, J.-X. Zhu, and E. Abrahams, Proc. Natl. Acad. Sci. U.S.A. **106**, 4118 (2009).
[3] Y. G. Naidyuk, O. E. Kvitnitskaya, N. V. Gamayunova, L. Boeri, S. Aswartham, S. Wurmehl, B. Büchner, D. V. Efremov, G. Fuchs, and S.-L. Drechsler, Phys. Rev. B **90**, 094505 (2014).
[4] K. Okazaki, Y. Ota, Y. Kotani, W. Malaeb, Y. Ishida, T. Shimojima, T. Kiss, S. Watanabe, C.-T. Chen, K. Kihou, C. H. Lee, A. Iyo, H. Eisaki, T. Saito, H. Fukazawa, Y. Kohori, K. Hashimoto, T. Shibauchi, Y. Matsuda, H. Ikeda, H. Miyahara, R. Arita, A. Chainani, and S. Shin, Science **337**, 1314 (2012).
[5] J.-P. Reid, M. A. Tanatar, A. Juneau-Fecteau, R. T. Gordon, S. R. de Cotret, N. Doiron-Leyraud, T. Saito, H. Fukazawa, Y. Kohori, K. Kihou, C. H. Lee, A. Iyo, H. Eisaki, R. Prozorov, and L. Taillefer, Phys. Rev. Lett. **109**, 087001 (2012).
[6] X. C. Hong, X. L. Li, B. Y. Pan, L. P. He, A. F. Wang, X. G. Luo, X. H. Chen, and S. Y. Li, Phys. Rev. B **87**, 144502 (2013).
[7] Z. Zhang, A. F. Wang, X. C. Hong, J. Zhang, B. Y. Pan, J. Pan, Y. Xu, X. G. Luo, X. H. Chen, and S. Y. Li, Phys. Rev. B **91**, 024502 (2015).
[8] F. Hardy, A. E. Böhmer, D. Aoki, P. Burger, T. Wolf, P. Schweiss, R. Heid, P. Adelmann, Y. X. Yao, G. Kotliar, J. Schmalian, and C. Meingast, Phys. Rev. Lett. **111**, 027002 (2013).
[9] A. F. Wang, B. Y. Pan, X. G. Luo, F. Chen, Y. J. Yan, J. J. Ying, G. J. Ye, P. Cheng, X. C. Hong, S. Y. Li, and X. H. Chen, Phys. Rev. B **87**, 214509 (2013).
[10] See Supplemental Material at http://link.aps.org/supplemental/10.1103/PhysRevLett.116.237003, which includes Refs. [11–27], for a description of the theoretical methods and experimental details.
[11] E. Fawcett *et al.*, *Electrons at the Fermi Surface*, edited by M. Springford (Cambridge University Press, Cambridge, 1980).
[12] B. Meyer, C. Elsässer, M. Lechermann, and F. Fähnle, *FORTRAN90: A Program for Mixed-Basis Pseudopotential Calculations for Crystals* (MPI für Metallforschung, Stuttgart, unpublished).
[13] R. Heid and K.-P. Bohnen, Phys. Rev. B **60**, R3709 (1999).
[14] M. Born and K. Huang, *Dynamical Theory of Crystal Lattices* (Oxford University Press, Oxford, 1954).
[15] R. Mittal, L. Pintschovius, D. Lamago, R. Heid, K.-P. Bohnen, D. Reznik, S. L. Chaplot, Y. Su, N. Kumar, S. K. Dhar, A. Thamizhavel, and T. Brueckel, Phys. Rev. Lett. **102**, 217001 (2009).
[16] D. Reznik, K. Lokshin, D. C. Mitchell, D. Parshall, W. Dmowski, D. Lamago, R. Heid, K.-P. Bohnen, A. S. Sefat, M. A. McGuire, B. C. Sales, D. G. Mandrus, A. Subedi, D. J. Singh, A. Alatas, M. H. Upton, A. H. Said, A. Cunsolo, Y. Shvyd'ko, and T. Egami, Phys. Rev. B **80**, 214534 (2009).
[17] C. Castellani, C. R. Natoli, and J. Ranninger, Phys. Rev. B **18**, 4945 (1978).
[18] R. Yu and Q. Si, Phys. Rev. Lett. **110**, 146402 (2013).
[19] T. Yoshida, S.-i. Ideta, I. Nishi, A. Fujimori, M. Yi, R. Moore, S.-K. Mo, D. Lu, Z.-X. Shen, Z. Hussain, K. Kihou, C. H. Lee, A. Iyo, H. Eisaki, and H. Harima, Front. Phys. **2**, 17 (2014).
[20] S. Kong, D. Y. Liu, S. T. Cui, S. L. Ju, A. F. Wang, X. G. Luo, L. J. Zou, X. H. Chen, G. B. Zhang, and Z. Sun, Phys. Rev. B **92**, 184512 (2015).
[21] P. Blaha, K. Schwarz, G. Madsen, D. Kvasnicka, and J. Luitz, *WIEN2k: An Augmented Plane Wave+Local Orbitals Program for Calculating Crystal Properties* (Karlheinz Schwarz, Techn. Universität Wien, Austria, Wien, 2001).
[22] S. Graser, A. F. Kemper, T. A. Maier, H.-P. Cheng, P. J. Hirschfeld, and D. J. Scalapino, Phys. Rev. B **81**, 214503 (2010).
[23] N. Marzari and D. Vanderbilt, Phys. Rev. B **56**, 12847 (1997).
[24] I. Souza, N. Marzari, and D. Vanderbilt, Phys. Rev. B **65**, 035109 (2001).
[25] S. Graser, T. A. Maier, P. J. Hirschfeld, and D. J. Scalapino, New J. Phys. **11**, 025016 (2009).
[26] J. Kuneš, R. Arita, P. Wissgott, A. Toschi, H. Ikeda, and K. Held, Comput. Phys. Commun. **181**, 1888 (2010).
[27] A. A. Mostofi, J. R. Yates, Y.-S. Lee, I. Souza, D. Vanderbilt, N. Marzari, A. A. Mostofi, J. R. Yates, Y.-S. Lee, I. Souza, D. Vanderbilt, and N. Marzari, Comput. Phys. Commun. **178**, 685 (2008).
[28] T. Terashima, N. Kurita, M. Kimata, M. Tomita, S. Tsuchiya, M. Imai, A. Sato, K. Kihou, C.-H. Lee, H. Kito, H. Eisaki, A. Iyo, T. Saito, H. Fukazawa, Y. Kohori, H. Harima, and S. Uji, Phys. Rev. B **87**, 224512 (2013).
[29] D. A. Zocco, K. Grube, F. Eilers, T. Wolf, and H. v. Löhneysen, Phys. Rev. Lett. **111**, 057007 (2013).

[30] D. A. Zocco, K. Grube, F. Eilers, T. Wolf, and H. v. Löhneysen, J. Phys. Soc. Jpn. Conf. Proc. **3**, 015007 (2014).
[31] D. Shoenberg, *Magnetic Oscillations in Metals* (Cambridge University Press, Cambridge, 1984).
[32] P. Burger, F. Hardy, D. Aoki, A. E. Böhmer, R. Eder, R. Heid, T. Wolf, P. Schweiss, R. Fromknecht, M. J. Jackson, C. Paulsen, and C. Meingast, Phys. Rev. B **88**, 014517 (2013).
[33] F. F. Tafti, J. P. Clancy, M. Lapointe-Major, C. Collignon, S. Faucher, J. A. Sears, A. Juneau-Fecteau, N. Doiron-Leyraud, A. F. Wang, X.-G. Luo, X. H. Chen, S. Desgreniers, Y.-J. Kim, and L. Taillefer, Phys. Rev. B **89**, 134502 (2014).
[34] J. Kanter, Z. Bukowski, J. Karpinski, and B. Batlogg, in *Annual Report of the Laboratory for Solid State Physics* (ETH Zürich, Department of Physics, Zürich, 2010).
[35] V. Taufour, N. Foroozani, M. A. Tanatar, J. Lim, U. Kaluarachchi, S. K. Kim, Y. Liu, T. A. Lograsso, V. G. Kogan, R. Prozorov, S. L. Bud'ko, J. S. Schilling, and P. C. Canfield, Phys. Rev. B **89**, 220509 (2014).
[36] L.-Y. T. Jian-Jun Ying, V. V. Struzhkin, H.-K. Mao, A. G. Gavriliuk, A.-F. Wang, X.-H. Chen, and X.-J. Chen, arXiv:1501.00330.
[37] S. Drotziger, P. Schweiss, K. Grube, T. Wolf, P. Adelmann, C. Meingast, and H. v. Löhneysen, J. Phys. Soc. Jpn. **79**, 124705 (2010).
[38] E. Granado, L. Mendon ça Ferreira, F. Garcia, G. d. M. Azevedo, G. Fabbris, E. M. Bittar, C. Adriano, T. M. Garitezi, P. F. S. Rosa, L. F. Bufaiçal, M. A. Avila, H. Terashita, and P. G. Pagliuso, Phys. Rev. B **83**, 184508 (2011).
[39] Z. P. Yin, K. Haule, and G. Kotliar, Nat. Mater. **10**, 932 (2011).
[40] T. T. Ong and P. Coleman, Phys. Rev. Lett. **108**, 107201 (2012).
[41] P. F. S. Rosa, T. M. Adriano, C. Garitezi, T. Grant, Z. Fisk, R. R. Urbano, and P. G. Pagliuso, Sci. Rep. **4**, 6543 (2014).
[42] K. Hashimoto, A. Serafin, S. Tonegawa, R. Katsumata, R. Okazaki, T. Saito, H. Fukazawa, Y. Kohori, K. Kihou, C. H. Lee, A. Iyo, H. Eisaki, H. Ikeda, Y. Matsuda, A. Carrington, and T. Shibauchi, Phys. Rev. B **82**, 014526 (2010).
[43] E. Abrahams and Q. Si, J. Phys. Condens. Matter **23**, 223201 (2011).
[44] L. Zhu, M. Garst, A. Rosch, and Q. Si, Phys. Rev. Lett. **91**, 066404 (2003).
[45] M. Garst and A. Rosch, Phys. Rev. B **72**, 205129 (2005).
[46] R. Yu, J.-X. Zhu, and Q. Si, Curr. Opin. Solid State Mater. Sci. **17**, 65 (2013).
[47] L. de' Medici, G. Giovannetti, and M. Capone, Phys. Rev. Lett. **112**, 177001 (2014).
[48] A. Georges, L. d. Medici, and J. Mravlje, Annu. Rev. Condens. Matter Phys. **4**, 137 (2013).
[49] S. Backes, H. O. Jeschke, and R. Valentí, Phys. Rev. B **92**, 195128 (2015).
[50] R. Yu and Q. Si, Phys. Rev. B **86**, 085104 (2012).
[51] J. G. Storey, J. W. Loram, J. R. Cooper, Z. Bukowski, and J. Karpinski, Phys. Rev. B **88**, 144502 (2013).
[52] P. Walmsley, C. Putzke, L. Malone, I. Guillamón, D. Vignolles, C. Proust, S. Badoux, A. I. Coldea, M. D. Watson, S. Kasahara, Y. Mizukami, T. Shibauchi, Y. Matsuda, and A. Carrington, Phys. Rev. Lett. **110**, 257002 (2013).
[53] Y. Nakajima, R. Wang, T. Metz, X. Wang, L. Wang, H. Cynn, S. T. Weir, J. R. Jeffries, and J. Paglione, Phys. Rev. B **91**, 060508 (2015).
[54] A. E. Böhmer, F. Hardy, L. Wang, T. Wolf, P. Schweiss, and C. Meingast, Nat. Commun. **6**, 7911 (2015).
[55] S. Kasahara, T. Shibauchi, K. Hashimoto, K. Ikada, S. Tonegawa, R. Okazaki, H. Shishido, H. Ikeda, H. Takeya, K. Hirata, T. Terashima, and Y. Matsuda, Phys. Rev. B **81**, 184519 (2010).
[56] L. E. Klintberg, S. K. Goh, S. Kasahara, Y. Nakai, K. Ishida, M. Sutherland, T. Shibauchi, Y. Matsuda, and T. Terashima, J. Phys. Soc. Jpn. **79**, 123706 (2010).
[57] P. Monthoux and D. J. Scalapino, Phys. Rev. Lett. **72**, 1874 (1994).
[58] T. Moriya and K. Ueda, Adv. Phys. **49**, 555 (2000).